

Changes in toughness at low oxygen concentrations in steel weld metals

S. Terashima* and H. K. D. H. Bhadeshia

Oxides in steel weld metals can initiate fracture or can improve toughness by influencing the development of beneficial microstructures. In this work, the authors conducted experiments in which the oxygen concentration was varied from 20 to 560 ppmw (parts per million by weight) in weld metals with tensile strength in the range 580–780 MPa. It is demonstrated that low and medium strength weld metals benefit from oxides up to a concentration of ~ 200 ppmw as consistent with previous research, because acicular ferrite is stimulated in the microstructure. By contrast, oxides are detrimental to the toughness of high strength weld deposits at low oxygen concentrations under 140 ppmw, because the microstructure remains a predominantly martensite and the oxides simply serve to nucleate fracture. In high strength weld metal, therefore, good toughness is achieved even at low oxygen concentration of 20 ppmw O.

Keywords: Charpy impact toughness, Weld metal, Oxygen, Oxide, Microstructure, CCT diagrams

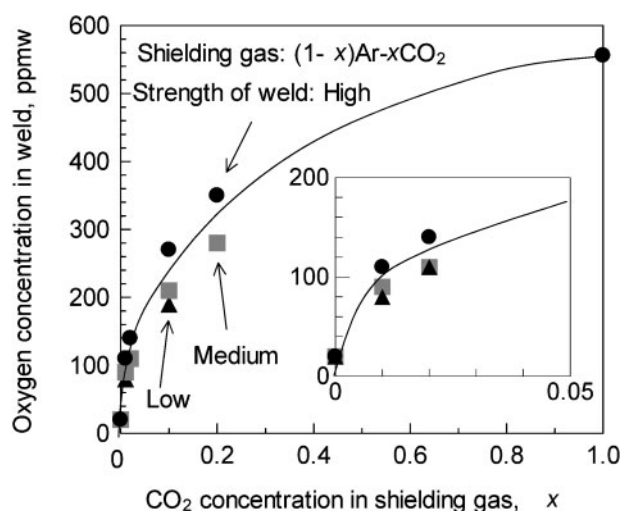
Introduction

The first indications that particle nucleated solid state transformations in steel welds can lead to an improvement in toughness came in the 1970s^{1–4} with indications that TiN precipitates stimulate the formation of acicular ferrite. This was soon followed by the discovery^{5,6} that it is oxide particles that play a key role in promoting acicular ferrite in weld deposits; this conclusion has been supported experimentally^{7–13} and the nature of acicular ferrite has also been investigated,^{14,15} although there remain diverse views on the atomic mechanisms of transformation.^{16–19} Ohkita and Horii have summarised the mechanisms by which acicular ferrite leads to better toughness,²⁰ essentially because its microstructure consists of a chaotic array of ferrite plates which frequently deflect cracks; this mechanism has been verified using orientation imaging methods.²¹

For weld metals with a tensile strength of ~ 500 MPa, a 200 ppmw of oxygen is said to be sufficient to ensure fine acicular ferrite, although the details depend on the oxide size distribution, chemical composition and the welding conditions;^{22–25} 'ppmw' refers to 'parts per million by weight'. Because concentrations in excess of this are found in most fusion welds, the focus on the design of tougher welds has been to reduce the level so as to avoid reaching levels where the benefit from acicular ferrite is overwhelmed by the presence of brittle oxides. In circumstances where the oxides cannot stimulate acicular ferrite (for example, in high hardenability weld metals with martensitic microstructures), calculations suggest that the toughness improves monotonically as the oxygen concentration is reduced, over a wide range

of 50–750 ppmw.²⁶ This has been demonstrated experimentally in strong (950 MPa) welds.²⁷

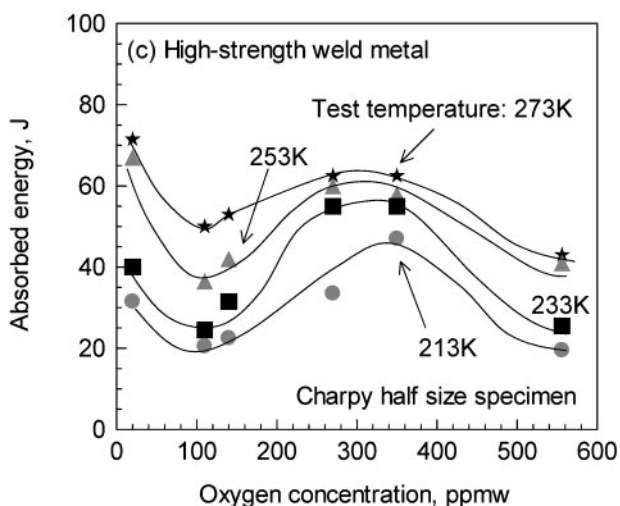
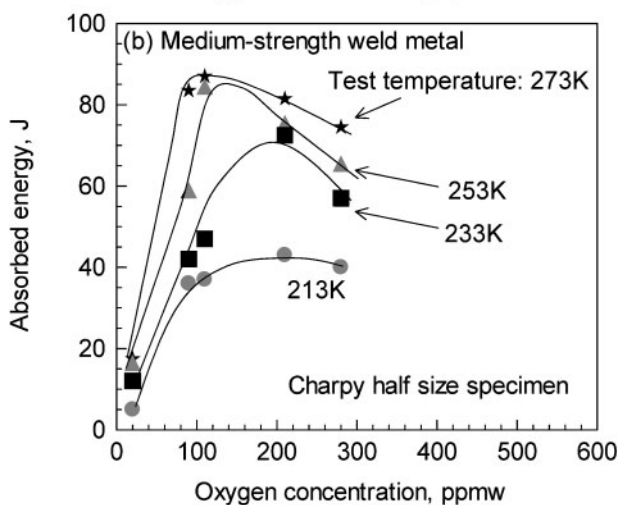
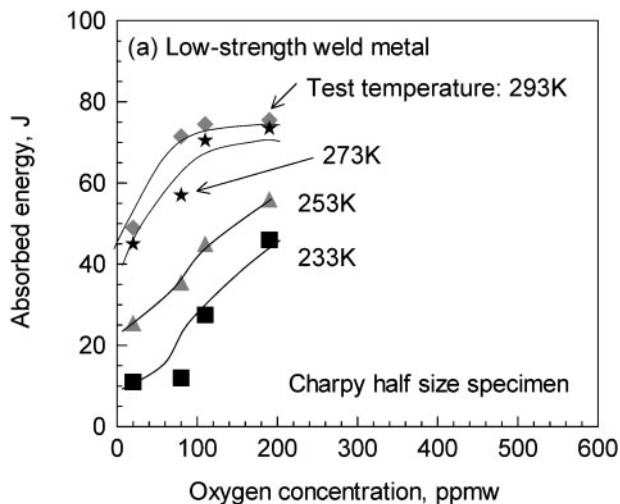
There is some mildly contradictory literature on intermediate strength weld metals (580–780 MPa). In some cases, it is found that the toughness increases as the oxygen concentration is reduced,^{28–31} whereas in others^{6,13,31,32} there appears to be a peak in toughness at ~ 200 ppmw of oxygen, attributed to an optimum oxide and acicular ferrite concentration. This class of weld metals is important from an engineering point of view, therefore the aim of this paper was to study the influence of oxygen at 20–600 ppmw on weld metals with tensile strength in the range 580–780 MPa, but with a particular focus on the higher strength welds. None of the above studies are as comprehensive in their coverage of oxygen concentration.



1 Relationship between oxygen concentration and shielding gas $(1-x)\text{Ar}-x\text{CO}_2$

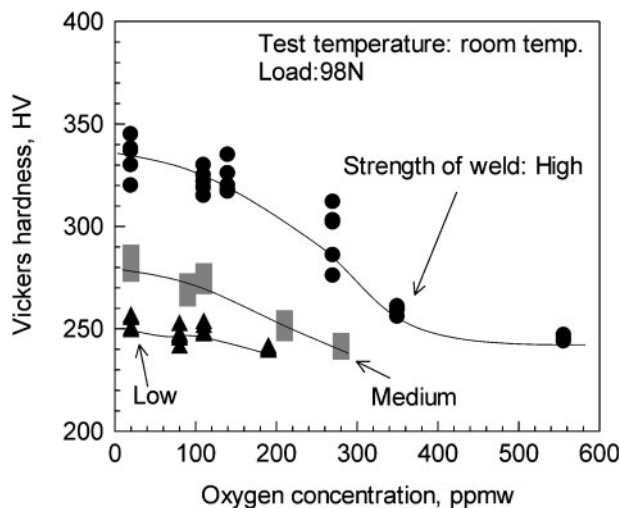
Materials Science and Metallurgy, University of Cambridge, Pembroke Street, Cambridge, CB2 3QZ, UK

*Corresponding author, email st379@cam.ac.uk



a low strength; b medium strength; c high strength

2 Charpy toughness as a function of oxygen concentration in different weld metals



3 Vickers hardness as function of oxygen concentration

Experimental

Welding conditions

Two 20 mm thick commercial steel plates with tensile strengths of 580 and 780 MPa, and corresponding commercial, 1.2 mm diameter wires were welded by the flat position metal active gas (MAG) shielded arc welding technique. Both the chemical compositions and the combinations of plates and wires used are shown in Tables 1 and 2 respectively. Edges of the plates to be single pass welded were prepared in a single V butt of 90° in angle. The nominal heat input was 3.4 kJ mm⁻¹, and the welding speed was 3.3 mm s⁻¹.

Metal active gas was chosen in order to achieve the required 20–600 ppmw of oxygen by controlling the composition of the shielding gas such as pure argon, 0.99Ar–0.01CO₂, 0.98Ar–0.02CO₂, 0.9Ar–0.1CO₂, 0.8Ar–0.2CO₂ and CO₂. Chemical compositions were evaluated by an inductively coupled plasma mass spectrometer (Table 3), with the exception of oxygen, which was determined using combustion analysis (Fig. 1).

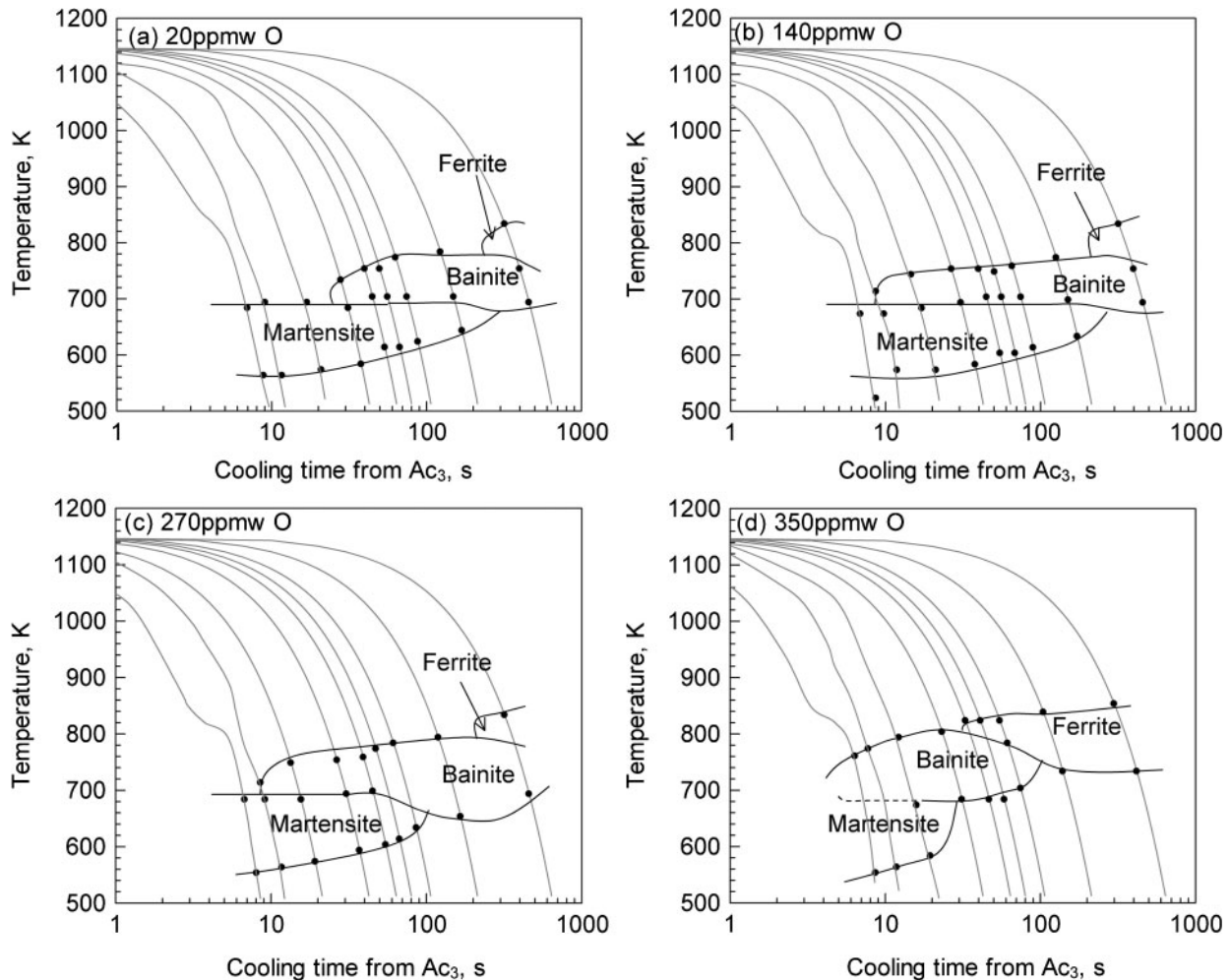
Dog bone type tensile samples with 6 mm diameter were machined from the weld metal parallel to the welding direction. The measured tensile strengths were found to be 624, 688 and 778 MPa for the three combinations of plate and wire. These are henceforth referred to as low, medium and high strength welds.

Toughness and microstructure

Half size (10 × 5 mm) rectangular Charpy V notch specimens were machined from the weld metal, with a 2 mm, 45° angle notch located within the weld metal. The fracture surfaces were characterised using scanning electron microscopy (SEM) and energy dispersive X-ray (EDX) analysis.

Table 1 Chemical compositions of plates and wires used, mass%

	C	Si	Mn	Cu	Ni	Cr	Mo	V	Nb	P	S
Plate (580MPa)	0.10	0.46	1.56	0.05	0.07	0.05	0.01	<0.01	<0.005	0.01	0.001
Wire (580MPa)	0.07	0.42	1.05	0.29	1.42	0.06	0.18	<0.01	<0.005	0.01	0.007
Plate (780MPa)	0.11	0.21	0.82	0.20	0.79	0.49	0.40	<0.01	<0.005	0.01	0.001
Wire (780MPa)	0.06	0.30	1.04	0.21	2.64	0.18	0.47	<0.01	<0.005	0.01	0.007

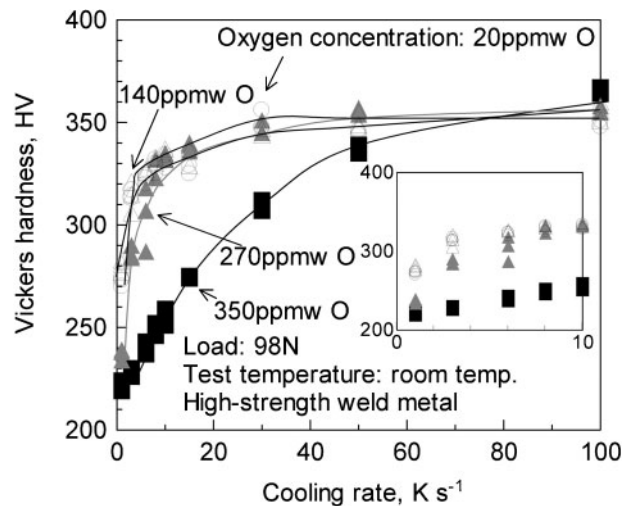


a 20 ppmw O; b 140 ppmw O; c 270 ppmw O; d 350 ppmw O
 4 CCT diagrams for high strength metal

The microstructure was characterised by both optical microscopy and SEM using metallographically prepared samples etched in 2% nital. Vickers hardness was measured on the metallographic samples using a 98 N load. Vickers microhardness test was also carried out with a load of 0.49 N. Crystallographic misorientations were determined on an orientation imaging microscope (OIM) equipped with a field emission gun, with a measuring step and area of 0.5 μm and 100 μm^2 respectively.

The volume fraction of acicular ferrite was measured using point counting on micrographs. The microhardness of each of the phases was established to obtain standard values. In some cases, there was doubt about the interpretation of the microstructure, in which the microhardness was measured and compared with the standard values to assist identification.

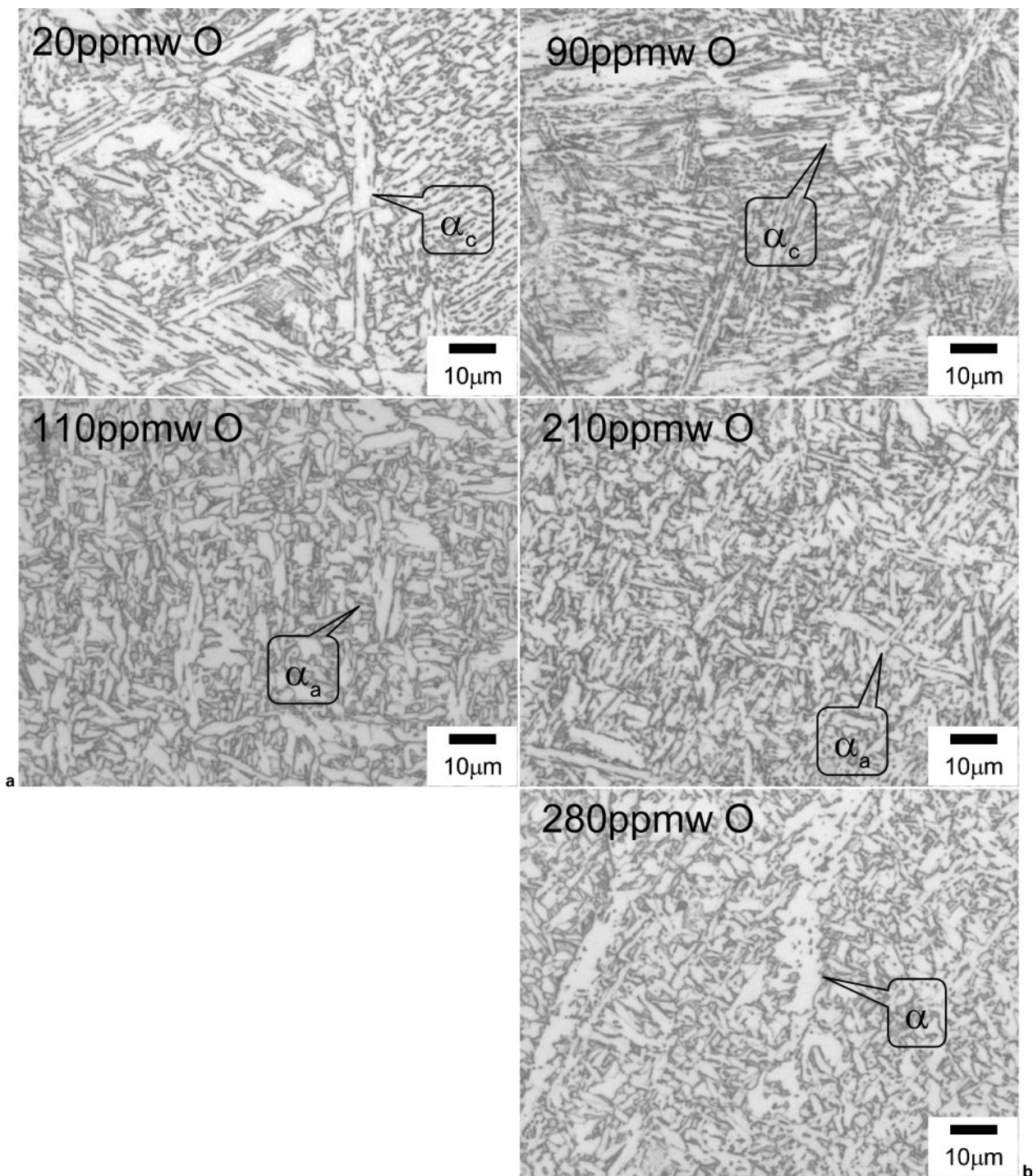
Continuous cooling transformation (CCT) diagrams were determined using high speed dilatometry on weld metal centreline samples machined well away from any diluted regions. The experiments were carried out in a



5 Vickers hardness of dilatometer samples used to generate diagrams in Fig. 4

Table 2 Combinations of plates and wires against target tensile strength in weld metals

Target tensile strength in weld metal, MPa	Nominal plate tensile strength, MPa	Nominal wire tensile strength, MPa
580	580	580
680	580	780
780	780	780

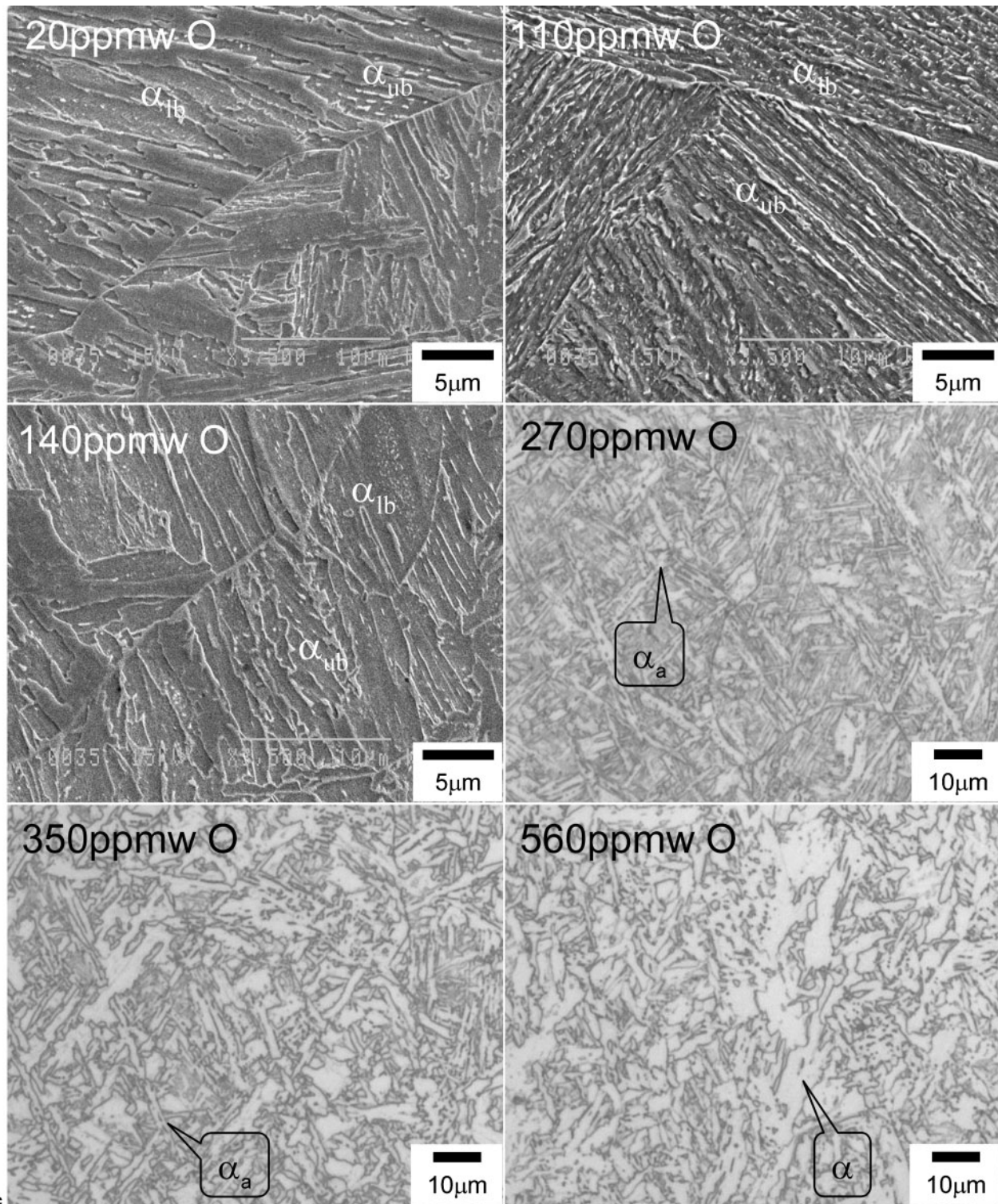


a low strength; b medium strength; c high strength

6 Micrographs of weld metals: α_c , α_a , α , α_{ub} and α_{lb} stand for coarsened structure, acicular ferrite, allotriomorphic ferrite, upper and lower bainite respectively

Table 3 Chemical compositions and shielding gas (1-x)Ar-xCO₂, mass%

MPa	x	C	Si	Mn	Cu	Ni	Cr	Mo	V	Nb	P	S
580	0	0.08	0.41	1.10	0.26	1.28	0.05	0.16	<0.01	<0.005	0.011	0.005
580	0.01	0.08	0.40	1.10	0.25	1.28	0.05	0.16	<0.01	<0.005	0.011	0.005
580	0.02	0.08	0.41	1.09	0.26	1.28	0.05	0.16	<0.01	<0.005	0.012	0.006
580	0.1	0.08	0.41	1.09	0.25	1.27	0.05	0.15	<0.01	<0.005	0.012	0.006
680	0	0.07	0.34	1.04	0.23	2.00	0.12	0.30	<0.01	<0.005	0.011	0.006
680	0.01	0.07	0.34	1.04	0.23	2.01	0.12	0.29	<0.01	<0.005	0.011	0.005
680	0.02	0.07	0.33	1.03	0.22	2.00	0.12	0.29	<0.01	<0.005	0.012	0.005
680	0.1	0.07	0.33	1.04	0.22	2.00	0.11	0.29	<0.01	<0.005	0.012	0.006
680	0.2	0.07	0.33	1.03	0.22	1.99	0.11	0.29	<0.01	<0.005	0.012	0.006
780	0	0.07	0.30	1.03	0.21	2.43	0.20	0.46	<0.01	<0.005	0.009	0.005
780	0.01	0.07	0.29	1.02	0.20	2.43	0.20	0.46	<0.01	<0.005	0.009	0.005
780	0.02	0.07	0.29	1.02	0.20	2.42	0.20	0.46	<0.01	<0.005	0.010	0.005
780	0.1	0.07	0.30	1.02	0.20	2.43	0.20	0.46	<0.01	<0.005	0.010	0.005
780	0.2	0.07	0.29	1.01	0.19	2.41	0.20	0.45	<0.01	<0.005	0.010	0.006
780	1	0.07	0.29	1.01	0.19	2.41	0.19	0.45	<0.01	<0.005	0.010	0.006



a low strength; b medium strength; c high strength

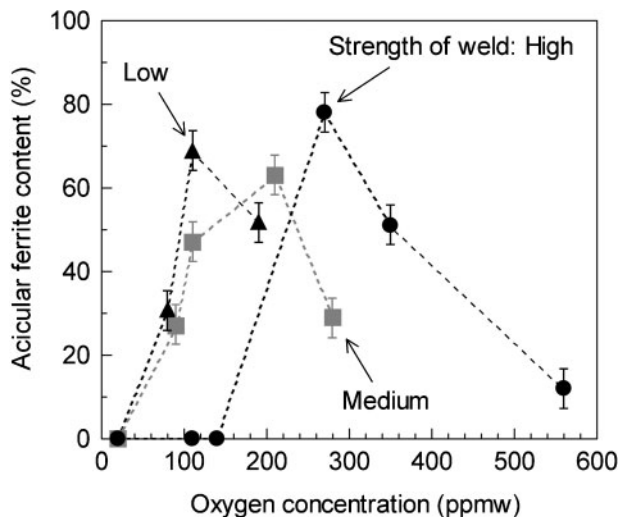
6 Micrographs of weld metals: α_c , α_a , α , α_{ub} and α_{ib} stand for coarsened structure, acicular ferrite, allotriomorphic ferrite, upper and lower bainite respectively

vacuum purged with pure argon at a pressure of 0.1 Pa. Austenitisation was at 1423 K for 300 s followed by cooling at 1, 3, 6, 8, 10, 15, 30, 50 and 100 K s⁻¹ in the range 1073–773 K.

Results and discussion

The toughness of the low strength deposit increased with oxygen concentration at all levels studied, up to 200 ppmw (Fig. 2a). The tests were carried out to a

greater concentration for the medium strength deposit, and revealed a peak in toughness as a function of the oxygen concentration (Fig. 2b). These observations for the low and medium strength alloys are as expected from the literature, because oxygen stimulates the formation of acicular ferrite (see metallographic results below). By contrast, the absorbed energy decreases up to 100 ppmw and then peaks at ~300 ppmw in the high strength alloy. It should be noted that good impact toughness is also achieved in high strength weld metal at 20 ppmw O,

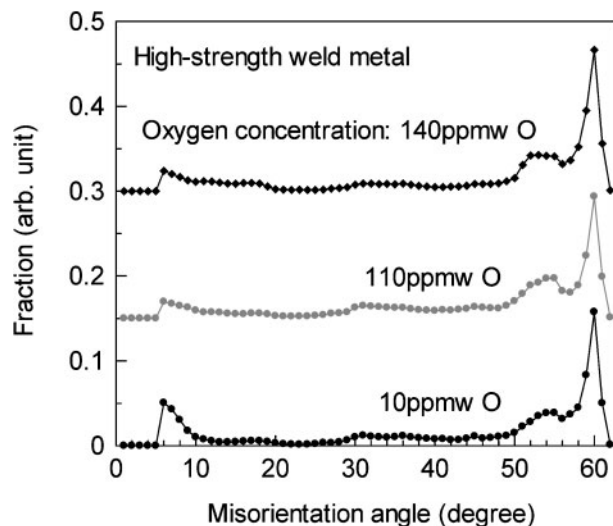


7 Acicular ferrite content as a function of oxygen concentration in low, medium and high strength weld metals

even though the oxygen concentration is low. The corresponding weld metal hardness data are illustrated in Fig. 3.

Ito *et al.* reported the acceleration of continuous cooling transformation diagram owing to oxygen in low strength (490 MPa) weld metals,²² but there are no similar reports for higher strength. Figure 4 shows a number of CCT diagrams for the present high strength weld. Both the bainite and ferrite regions are accelerated as the oxygen concentration is increased, indicating the role of oxides in providing additional heterogeneous nucleation sites. This is consistent with the decrease in weld metal hardness (Fig. 3) and in the dilatometer sample hardness (Fig. 5) as the oxygen is increased; these results are also consistent with the low strength weld data reported by Ito *et al.*²² The authors were not able to measure the columnar austenite grain size of the present high strength weld. It is possible that the austenite grains are coarser for the lower oxygen concentrations, contributing to the increase in hardenability at low concentrations. However, the columnar austenite grains evolve from delta-ferrite, and the oxide particles are then unlikely to pin transformation interfaces.¹⁶ It is likely, therefore, that observed changes in transformation kinetics are largely owing to the role of oxides in increasing the number density of nucleation sites.

Figure 6 shows the microstructure of the *a* low and *b* medium strength welds, where α_c , α_a and α stand for 'coarse structure' (clusters of similarly oriented Widmanstätten ferrite), acicular ferrite and allotriomorphic ferrite respectively. Fine acicular ferrite structures were observed at the intermediate oxygen level of 110 and 210 ppmw O, while the coarse structures appeared at 20 and 90 ppmw O for the low and medium strength alloys respectively. Furthermore, coarse allotriomorphic ferrite appeared at the high oxygen of 280 ppmw O in the medium strength weld metal (Fig. 6*b*). The general result from the metallography is that acicular ferrite is optimised in the low and medium strength deposits for oxygen concentrations of ~200 ppmw as shown in Fig. 7. This explains the observed increase in toughness (Fig. 2*a* and *b*). As

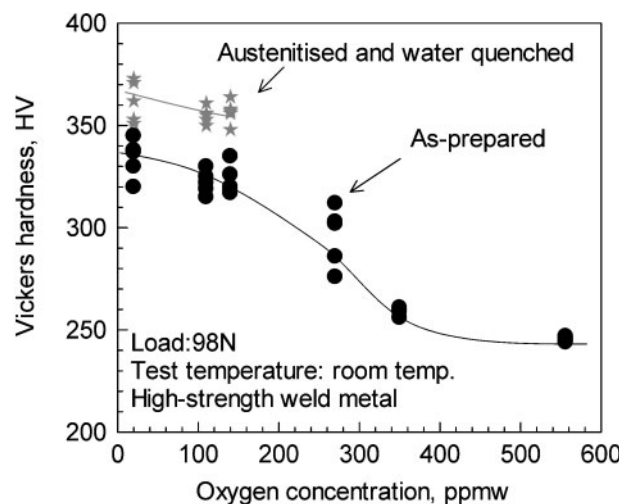


8 Crystallographic misorientation distribution for high strength weld metal with 20, 110 and 140 ppmw O

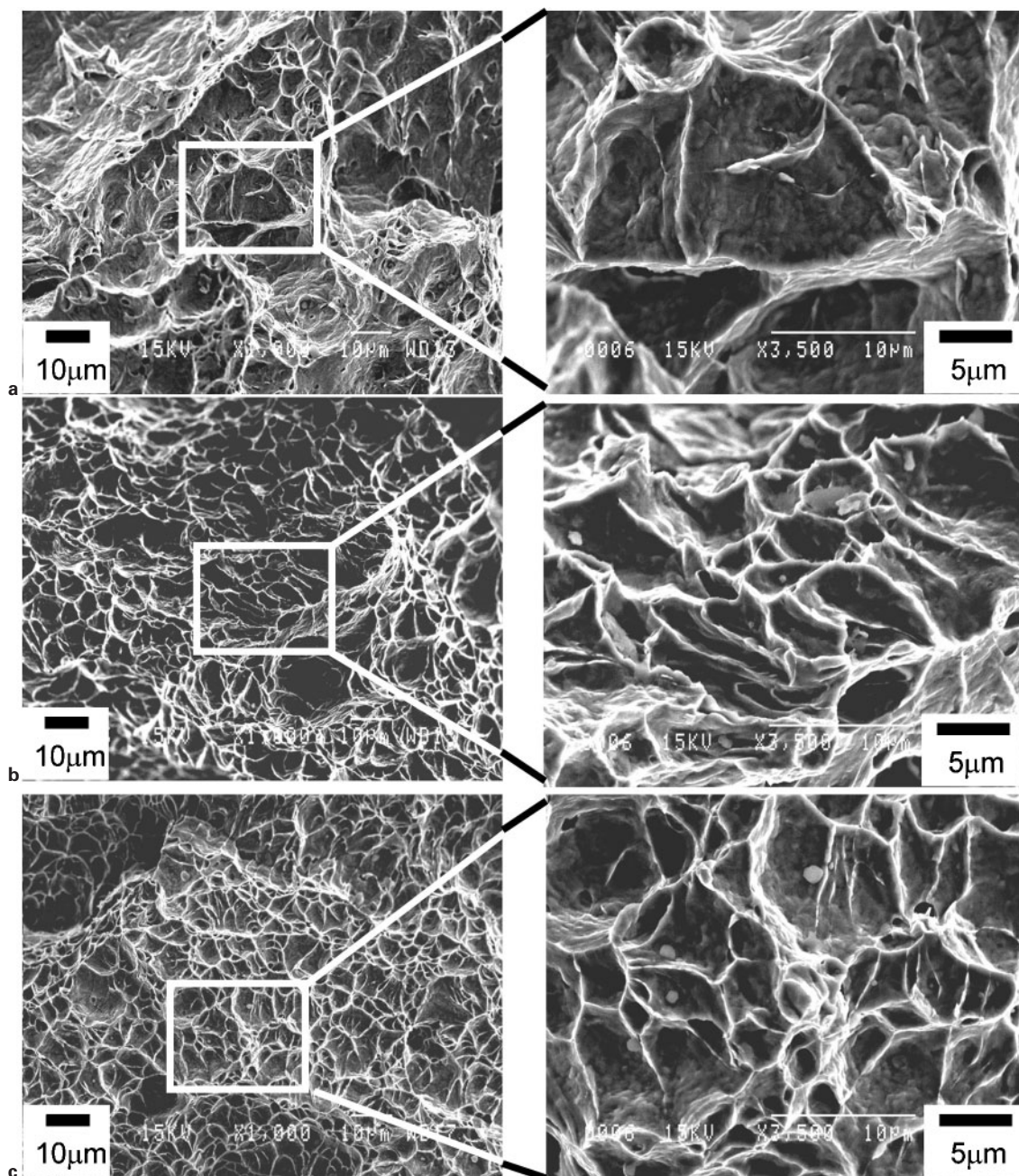
mentioned above, the medium strength weld demonstrates that coarser microstructures form at higher oxygen concentration of 280 ppmw, so that toughness deteriorates in spite of the decrease in hardness. Of course, the large concentration of inclusions must also lead to a decrease in toughness.

This last point is emphasised by the results on the high strength welds shown in Fig. 6*c*, where impact toughness is also high at the low oxygen concentration of 20 ppmw O and then decreases with oxygen concentration up to 140 ppmw (Fig. 2*c*) in spite of the decrease in hardness (Fig. 3), because of the absence of acicular ferrite (Fig. 7). The high hardenability means that the microstructure is dominated by classical grain boundary nucleated upper and lower bainite, α_{ub} and α_{lb} respectively, along with martensite.

Gourgues *et al.* have pointed out that crystallographic misorientation distribution for both lower bainite and martensite structure has a single strong peak and a small peak at 53–60°, whereas two strong peaks appear at 52–53° and ~60° for upper bainite and ferrite.²¹ The results



9 Vickers hardness for austenitised and water quenched samples of high strength weld metal with 20, 110 and 140 ppmw O; weld metal data are included for comparison



a 20 ppmw O; b 110 ppmw O; c 140 ppmw O
10 Fractographs of high strength weld metal

in Fig. 8 confirm that for oxygen concentrations 20–140 ppmw, the misorientations obtained are consistent with a microstructure dominated by martensite with lower bainite.

The hardness data can be further interpreted by establishing that of 100% martensite. A sample of the high strength alloy with 20, 110 and 140 ppmw O was austenitised at 1173 K for 300 s and rapidly quenched into water. Figure 9 shows that the high strength welds with oxygen up to 140 ppmw contain a substantial amount of martensite, consistent with the reduction in toughness as the oxygen concentration increases. The slight decrease in hardness as the oxygen is increased from 20 to 140 ppmw is due to an increase in bainite at the expense of martensite, consistent with the dilatometer data.

Figure 10 shows fracture surfaces of Charpy samples from the high strength weld (20–140 ppmw O). It is

evident that the dimple size decreases as the oxygen concentration increases, a reflection of the larger number density of void nucleation sites.^{23,26} These observations explain the decrease in impact energy up to 140 ppmw O at all test temperatures, consistent with previous work on inclusions >1 μm (Ref. 33).

It is not surprising that the impact toughness of the high strength weld at the highest oxygen concentration (560 ppmw) is poor. For 270–350 ppmw O, acicular ferrite appeared in the high strength weld (Fig. 6c), giving rise to the peak in toughness.

Summary

Consistent with previous work, it is found that the introduction of oxides during the deposition of low and medium strength welds stimulates the formation of acicular ferrite, and hence leads to an improvement in

toughness. Beyond an optimum concentration, the toughness then deteriorates as the benefit from an improved microstructure is overwhelmed by the initiation of fracture at non-metallic inclusions.

The relationship between toughness and oxygen concentration is different for high hardenability (high strength) welds, where the microstructure at low oxygen concentrations is dominated by martensite and bainite. The toughness is also high at the low oxygen concentration of 20 ppmw O and then decreases as the oxygen concentration increases, because acicular ferrite is absent from the microstructure, so that oxides simply serve to nucleate fracture.

The oxides do accelerate transformation, therefore at much higher concentrations of oxygen, acicular ferrite is eventually stimulated even in high hardenability welds, leading to an increase in toughness. Very high oxygen concentrations contribute to a subsequent reduction in toughness.

Acknowledgements

The authors are grateful to Dr R. J. Pargeter, Dr D. J. Abson, Dr P. H. M. Hart and Dr G. Wylde for valuable discussions and the provision of laboratory facilities at TWI (England), and Mr J. S. Bates and Professor R. C. Thomson for access to EBSD facilities in Loughborough University (England). This work was financially supported by Nippon Steel Corporation (Japan).

References

1. Y. Ito and M. Nakanishi: *J. Jpn. Weld. Soc.*, 1975, **44**, 815–821.
2. Y. Ito and M. Nakanishi: *Sumitomo Search*, 1976, **15**, 42–62.
3. S. Kanazawa, A. Nakashima, K. Okamoto and K. Kanaya: *Trans. Iron Steel Inst. Jpn.*, 1976, **16**, 486–495.
4. T. H. North, H. B. Bell, A. Koukabi and I. Craig: *Weld. J.*, 1979, **58**, S343–S354.
5. D. J. Abson, R. E. Dolby and P. H. M. Hart: Proc. Int. Conf. on 'Trends in steel and consumables for welding', London, UK, November 1978, The Welding Institute, 75–101.
6. H. Terashima and J. Tsuboi: Proc. Natl Meet. JWS '78, Tokyo, Japan, April 1978, Japan Welding Society, 28–29.
7. I. Watanabe and T. Kojima: *J. Jpn. Weld. Soc.*, 1980, **49**, 772–780.
8. I. Watanabe and T. Kojima: *J. Jpn. Weld. Soc.*, 1981, **50**, 778–786.
9. N. Mori, H. Homma, S. Ohkita and M. Wakabayashi: *J. Jpn. Weld. Soc.*, 1981, **50**, 175–181.
10. P. L. Harrison and R. A. Farrar: *J. Mater. Sci.*, 1981, **16**, 2218–2226.
11. M. Ferrante and R. A. Farrar: *J. Mater. Sci.*, 1982, **17**, 3293–3298.
12. R. A. Ricks, P. R. Howell and G. S. Barritte: *J. Mater. Sci.*, 1982, **17**, 732–740.
13. H. Terashima and J. Tsuboi: *Met. Constr.*, 1982, **14**, 648–654.
14. H. K. D. H. Bhadeshia, L.-E. Svensson and B. Gretoft: *Acta Metall.*, 1985, **7**, 1271–1283.
15. S. S. Babu and H. K. D. H. Bhadeshia: *Mater. Sci. Technol.*, 1990, **6**, 1005–1020.
16. H. K. D. H. Bhadeshia and L.-E. Svensson: in 'Mathematical modelling of weld phenomena', (ed. K. E. Easterling and H. Cerjak), 109–182; 1993, London, The Institute of Materials.
17. H. K. D. H. Bhadeshia: 'Bainite in steels', 2nd edn, 237–276; 2001, London, IOM Communications.
18. G. Thewlis: *Mater. Sci. Technol.*, 2004, **20**, 143–160.
19. T. Koseki and G. Thewlis: *Mater. Sci. Technol.*, 2005, **21**, 867–879.
20. S. Ohkita and Y. Horii: *ISIJ Int.*, 1995, **35**, 1170–1182.
21. A.-F. Gourgues, H. M. Flower and T. C. Lindley: *Mater. Sci. Technol.*, 2000, **16**, 26–40.
22. Y. Ito, M. Nakanishi and Y. Komizo: *Met. Constr.*, 1982, **14**, 472–478.
23. Y. Sato, N. Hayakawa and T. Kuwana: *Q. J. Jpn. Weld. Soc.*, 1992, **10**, 422–428.
24. M. I. Onsoien, S. Liu and D. L. Olson: *Weld. J.*, 1996, **75**, S216–S224.
25. R. P.-Cvetkovic, A. Milosavljevic, A. Sedmak and O. Popovic: *J. Serb Chem Soc.*, 2006, **71**, 313–321.
26. E. A. Metzbower, J. J. DeLoach, S. H. Lalam and H. K. D. H. Bhadeshia: *Sci. Technol. Weld. Join.*, 2001, **6**, 368–374.
27. M. Gouda, M. Takahashi and K. Ikeuchi: *Sci. Technol. Weld. Join.*, 2005, **10**, 369–377.
28. K. Shinada, Y. Horii and N. Yurioka: *Weld. J.*, 1992, **71**, S253–S262.
29. G. L. F. Powell and G. Herfurth: *Metall. Mater. Trans. A*, 1998, **29A**, 2775–2784.
30. B. Utterberg and L.-E. Svensson: *Sci. Technol. Weld. Join.*, 2002, **7**, 363–373.
31. N. M. Ramini de Rissone, I. de S. Bott, L. A. de Vedia and E. S. Surian: *Sci. Technol. Weld. Join.*, 2003, **8**, 113–122.
32. H. Terashima and P. H. M. Hart: *Weld. J.*, 1984, **63**, S173–S183.
33. S. Ohkita, H. Homma, S. Tsushima and N. Mori: *Austr. Weld. J.*, 1984, **29**, 29–36.
34. J. H. Tweed and J. F. Knott: *Acta Metall.*, 1987, **35**, 1401–1414.